Pair-Breaking and Superconducting State Recovery Dynamics in MgB_2

J. Demsar,[1,2] R. D. Averitt,[1] A. J. Taylor,[1] V. V. Kabanov,[2] W. N. Kang,[3] H. J. Kim,[3] E. M. Choi,[3] and S. I. Lee[3]

[1]*Los Alamos National Laboratory, MST-10, Los Alamos, New Mexico 87545, USA*

[2]*"J. Stefan" Institute, Jamova 39, Ljubljana, Slovenia*

[3]*National Creative Research Initiative Center for Superconductivity, Department of Physics, Pohang University of Science and Technology, Pohang 790-784, Korea*

(Received 16 May 2003; published 29 December 2003)

We present studies of the photoexcited quasiparticle dynamics in MgB_2 where, using femtosecond optical techniques, Cooper pair-breaking dynamics (PBD) have been temporally resolved for the first time. The PBD are strongly temperature and photoexcitation intensity dependent. Analysis of the PBD using the Rothwarf-Taylor equations suggests that the anomalous PBD arises from the fact that in MgB_2 photoexcitation is initially followed by energy relaxation to high frequency phonons instead of, as commonly assumed, *e-e* thermalization. Furthermore, the bare quasiparticle recombination rate and the probability for pair breaking by phonons have been determined.

DOI: 10.1103/PhysRevLett.91.267002 PACS numbers: 74.25.Gz, 74.40.+k, 78.47.+p

Recently, femtosecond spectroscopy has been shown to present an excellent experimental alternative for studying temperature (T) dependent changes in the low energy electronic structure of correlated electron systems [1–8]. In these experiments, a femtosecond laser pump pulse excites electron-hole pairs via an interband transition. In a process which is similar in many materials including metals and superconductors (SC), these hot carriers rapidly thermalize via electron-electron (*e-e*) and electron-phonon (*e*-ph) collisions reaching states near the Fermi energy within 10–100 fs. The subsequent relaxation and recombination dynamics (strongly affected by the opening of the superconducting [1–5] or charge density wave [6] gap) are observed either by measuring photo-induced (PI) changes in reflectivity or transmission at optical frequencies [1–4,6], or by measuring conductivity dynamics at terahertz (THz) frequencies [5]. While high-temperature superconductors have been extensively studied over the last decade or so [1–5], the data on more conventional BCS-type superconductors are limited [9,10]. To our knowledge, no systematic study of photoexcited quasiparticle (QP) dynamics with femtosecond resolution has been performed on low-T_c superconductors.

In this Letter, we present the first femtosecond time-resolved study of photoexcited carrier dynamics in the recently discovered superconductor MgB_2, utilizing both optical pump-THz probe (OPTP) and optical pump-optical probe (OPOP) techniques. The aim of this study is to elucidate the photoexcited carrier dynamics in MgB_2 and in SC's in general and to obtain new and complementary knowledge of the electronic structure of MgB_2. The discovery of superconductivity below 39 K in MgB_2 [11] has generated a great deal of excitement since T_c is higher by nearly a factor of 2 in comparison to other previously known simple intermetallic SC's. While the observation of a significant boron isotope effect [12] and the spin-singlet nature of the pairing [13] indicate conventional phonon mediated pairing in MgB_2, several experimental [14–16] and theoretical studies [17–19] suggest the presence of two distinct energy gaps [14].

Since the SC gaps in MgB_2 lie in the THz range [20], OPTP spectroscopy is well suited to study the dynamics of PI quasiparticles. In particular, the Cooper pair-breaking dynamics (PBD) have been time resolved for the first time. The PBD are temperature and photoexcitation fluence dependent. This is attributed to an initial strong relaxation to high frequency phonons and supported by detailed analysis using the Rothwarf-Taylor model [21]. The SC state recovery dynamics proceed on the time scale of hundreds of picoseconds. Systematic studies as a function of temperature, excitation intensity, and film thickness suggest that pair recovery is governed by the anharmonic decay of 2Δ acoustic phonons.

In time-domain THz spectroscopy a nearly single-cycle electric field transient, containing Fourier components from ~100 GHz to several THz, is generated via optical rectification of 150 fs optical pulses in a ZnTe crystal. The THz electric field transmitted through a sample, $E_{\mathrm{sam}}(t)$, is detected using the Pockels effect in ZnTe [5,7]. A measurement of the transmitted electric field is also made using a suitable reference, $E_{\mathrm{ref}}(t)$, which, for these experiments, is a blank sapphire substrate. Dividing the Fourier transforms of the sample and reference data gives the complex transmissivity $T(\omega) = E_{\mathrm{sam}}(\omega)/E_{\mathrm{ref}}(\omega)$. The real and imaginary conductivities $[\sigma_r(\omega),\ \sigma_i(\omega)]$ of the film are determined using the appropriate Fresnel equation, without the need for Kramers-Kronig analysis [22]. For the OPTP experiments, the induced change in the transmitted electric field, $\Delta E_{\mathrm{sam}}(t)$, is measured as a function of time delay with respect to an optical excitation pulse. From $\Delta E_{\mathrm{sam}}(t)$, it is then possible to determine the PI change of $\sigma(\omega)$ with picosecond (ps) resolution [7,23,24].

The OPTP experiments were performed on 80 and 100 nm MgB_2 thin films ($T_c \sim 34$ K) on sapphire [25], whereas the films used in OPOP experiments had thicknesses of 300 and 400 nm, and $T_c = 39$ K. Further details of the film growth [25] and a detailed description of experimental techniques are given elsewhere [1,2,5]. The photoexcitation fluence F ranged from 0.1–5 μJ/cm^2, corresponding [26] to an absorbed energy density $\Omega =$ 2–110 μeV/unit cell. For comparison, Ω corresponding to the complete destruction of the SC state was found to be ≈ 110 μeV/unit cell, in agreement with the condensation energy in the BCS limit [26].

Figure 1 shows $\sigma_i(\omega)$ and $\sigma_r(\omega)$ at several time delays after photoexcitation with a 150 fs pulse with $F \sim 3$ μJ/cm^2. Since σ_i provides a direct probe [22] of the condensate density, n_s, by measuring PI changes in σ_i direct information of n_s dynamics can be extracted. On the other hand, the increase and subsequent recovery of $\sigma_r(\omega)$ corresponds to an initial increase in the number of QPs followed by their recombination [5]. The decrease of $\sigma_i(\omega)$—corresponding to a reduction of n_s—occurs on the time scale of several ps, followed by recombination dynamics on the time scale of several hundred ps. To obtain a more detailed time evolution of the PI changes in $\sigma(\omega)$, we utilize the fact that the induced changes in the electric field transient, ΔE_{sam}, are mainly due to a phase shift of the electric field; see the inset of Fig. 1(a). The origin of the phase shift is the so-called kinetic inductance due to SC pairing, i.e., the conductivity due to the SC pairs is purely imaginary with a $1/\omega$ dependence resulting in the overall phase shift in $E_{\mathrm{sam}}(t)$ below T_c. When F is smaller than the fluence corresponding to destruction of the SC state, $\Delta E_{\mathrm{sam}}(t = t_0)$ [t_0 is a fixed point of $E_{\mathrm{sam}}(t)$ which, for these experiments, was at the point of maximum time derivative of the electric field, indicated by the arrow in the inset of Fig. 1(a)] is proportional to the PI conductivity $\Delta\sigma$ [both $\Delta\sigma_i$ and $\Delta\sigma_r$ have the same dynamics; see the inset of Fig. 1(b)]. Therefore by measuring $\Delta E_{\mathrm{sam}}(t = t_0)$ while scanning the pump line, the PI conductivity dynamics $\Delta\sigma(t)$ can be extracted rapidly and with much higher temporal resolution.

Figure 2(a) presents the induced conductivity dynamics as a function of T ($F \approx 1$ μJ/cm^2). The relaxation time τ_R, obtained by fitting the data to $\exp(-t/\tau_R)$, shows a pronounced T dependence, plotted by circles in the inset of Fig. 2(a). Upon increasing T, τ_R first decreases, reaching a minimum, followed by a quasidivergence as T_c is approached. Similar results are obtained from the OPOP experiments, Fig. 2(b), where PI changes in reflectivity ($\Delta R/R$) as optical frequencies are measured (20 fs pulses at $\hbar\omega \approx 1.54$ eV have been used as a source of both pump and probe pulses). The normal state dynamics [27] are characterized by a resolution limited rise time (40 fs), followed by a two-exponential decay, with decay times $\tau_1 \approx 0.15$ ps and $\tau_2 \approx 3.5$ ps. After the initial ps dynamics, $\Delta R/R$ changes sign and the recovery dynamics proceed on a time scale longer than 1 ns. Below T_c, however, an additional subnanosecond response becomes evident, whose amplitude and recovery dynamics is strongly T dependent [28]. In particular, the T dependence of τ_R, plotted in the inset of Fig. 2(b), displays the same T dependence as the OPTP data.

The SC state recovery dynamics do not show any dependence on F in the range $0.1 < F < 5$ μJ/cm^2. This suggests that the SC recovery dynamics are governed by the phonon-bottleneck mechanism, proposed by Rothwarf and Taylor [21] (biparticle recombination should be intensity dependent). In this case recovery dynamics are governed by the lifetime of $\omega \gtrsim 2\Delta$ phonons, which are in thermal equilibrium with QPs [21]. Since in MgB_2 2Δ is much smaller than the energy of the lowest optical phonon mode ($\approx$40 meV) [29], the SC

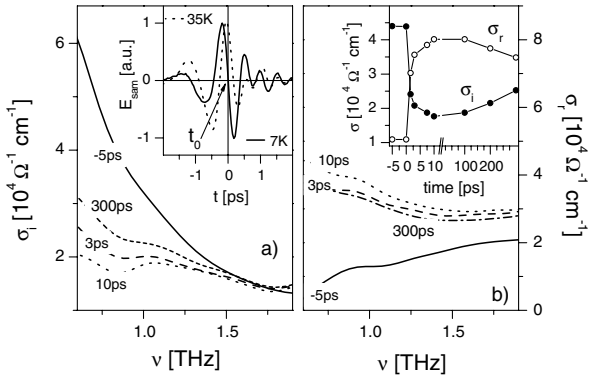

FIG. 1. The (a) imaginary and (b) real conductivities as a function of frequency shown at various time delays following excitation with a fluence $F \sim 3$ μJ/cm^2 at 7 K. Inset of (a): $E_{\mathrm{sam}}(t)$ at 7 and 35 K. Inset of (b): the time evolution of σ_r and σ_i taken at $\nu = 0.8$ THz.

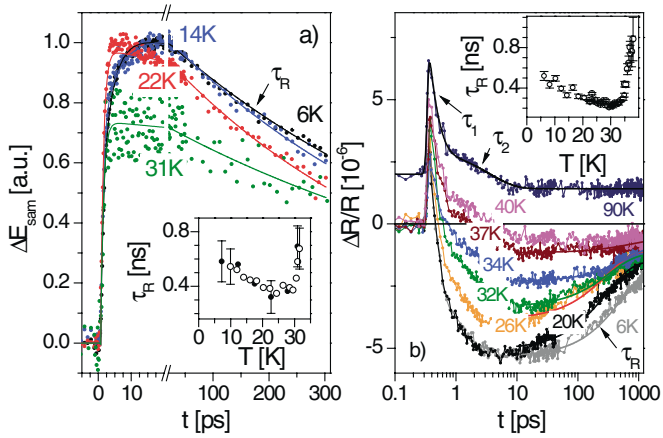

FIG. 2 (color online). (a) The PI change in conductivity ($\Delta\sigma \propto \Delta E_{\mathrm{sam}}$) as a function of temperature. (b) The PI reflectivity traces at various temperatures plotted on a semilog scale. The normal state trace (90 K) is vertically shifted for clarity. The T dependence of the superconducting state recovery time, τ_R, determined by single exponential fits to the data (solid lines) is presented in the insets.

recovery is governed by the decay of acoustic phonons. The decay of $\omega \gtrsim 2\Delta$ phonon population is governed either by anharmonic decay to $\omega < 2\Delta$ phonons or escape of $\omega \gtrsim 2\Delta$ phonons to the substrate [28]. The fact that no change in τ_R is observed when comparing the data taken on 80, 100, and 400 nm films suggests that in MgB_2 the predominant mechanism that governs the SC condensate recovery is anharmonic phonon decay. This assignment is further supported by the observed T dependence of τ_R, which near T_c shows [1] $\tau_R \propto 1/\Delta(T)$ and the estimated anharmonic decay time of the 10 meV longitudinal acoustic phonon in MgB_2 of ≈ 1 ns [26].

When discussing the OPOP data we should mention the peculiar ps normal state dynamics, present also in the SC state. In metals, ps QP dynamics are usually interpreted in terms of the two-temperature model (TTM) [8,30,31]. Here the assumption that the e-e scattering is much faster than e-ph scattering leads to the description of the PI transient in terms of the time evolution of the electronic temperature T_e, i.e., $\Delta R(t) = \partial R/\partial T\ \Delta T_e(t)$. The recovery dynamics are due to e-ph thermalization which is proportional to the e-ph coupling constant λ [8,31]. For MgB_2, however, the ps dynamics are inconsistent with the TTM since (i) the $\Delta R/R$ transient changes sign with time [27]; (ii) $\partial R/\partial T$ at 1.5 eV is negative [32], so $\Delta R/R < 0$ in the TTM, contrary to what is observed; (iii) the expected e-ph thermalization time [33] is $\tau_{ep} \approx 20fs$, which is much shorter than the experimental values of either τ_1 or τ_2; and (iv) the initial dynamics do not change upon cooling below T_c, where the bottleneck in the relaxation due to the presence of the SC gap should strongly affect the recovery dynamics [1,21]. The above arguments suggest that the origin of the ps dynamics measured in OPOP experiments is not associated with e-ph thermalization and indicates that the assumption of e-e thermalization being much faster than the e-ph scattering is invalid in MgB_2. Since the coupling between electrons and high frequency optical phonons in MgB_2 is very strong (in particular the coupling of σ band electrons to the E_{2g} phonon mode at 60–80 meV) [18,19,34], it is quite possible that the situation in MgB_2 is reversed (or at least that the two time scales are comparable). In this scenario the initial relaxation of photoexcited electrons proceeds via emission of high frequency (60–80 meV) optical phonons which only subsequently release their energy to the electron system via phonon-electron scattering, and to low energy phonons via anharmonic decay. We believe that the ps dynamics observed in OPOP experiments is due to the energy relaxation of the optical phonon population, rather than e-ph thermalization.

Finally, let us discuss the rise-time dynamics, reflecting the Cooper pair-breaking processes (i.e., the initial reduction of n_s). Figure 2(a) and the inset of Fig. 1(b) clearly show a finite rise time in the induced change in conductivity, indicating that it takes some time for the completion of pair breaking following optical excitation. Furthermore, Fig. 2(a) shows that the PBD are T dependent (the PBD becomes faster as T is increased). Also, the PBD depend on the photoexcitation intensity. Figure 3(a) shows the early time $\Delta\sigma(t)$ taken at 7 K for different fluences. While the solid symbols represent the data obtained by measuring $\Delta E_{sam}(t)$, the open symbols represent the induced change in the conductivity obtained directly using the two-dimensional scanning technique. The agreement between the two data sets clearly shows that the phase changes accurately reveal the condensate dynamics. This is particularly important, since measuring $\Delta E_{sam}(t)$ enables the study of condensate dynamics with subpicosecond resolution (limited by optical pulse widths to ≈ 0.3 ps), while the two-dimensional scanning technique is limited by the THz pulse width (~ 2 ps) [24].

In view of the normal state OPOP data, which suggest that high energy electrons initially release most of their energy via emission of high frequency phonons (which subsequently break Cooper pairs), there is a natural explanation of the observed fluence and T dependence of the PBD in MgB_2 [28]. To show this, we consider the Rothwarf-Taylor model, where the dynamics of the QP and high frequency ($\omega > 2\Delta$) phonon densities, n and N, are described by a set of two coupled differential equations [21]. Since the SC recovery dynamics proceed on a much longer time scale than the PBD, the term describing the loss of $\omega > 2\Delta$ phonons by processes other than pair excitation can be neglected, and the equations are

$$dn/dt = \beta N - Rn^2; \qquad dN/dt = \frac{1}{2}[Rn^2 - \beta N]. \quad (1)$$

Here R is the bare quasiparticle recombination rate and β is the probability for pair breaking by phonons [21]. With the initial condition that after photoexcitation (and initial subpicosecond e-e and e-ph dynamics) the QP and high

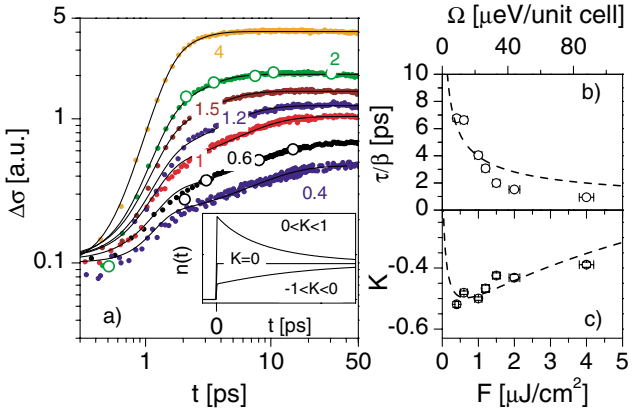

FIG. 3 (color online). (a) The rise time dynamics at 7 K taken at various F in $\mu J/cm^2$ (for presentation purpose all traces have been shifted vertically by 0.1). Solid circles represent the data obtained by scanning the pump line while measuring $\Delta E(t = t_0)$, while the open circles correspond to $\Delta\sigma$ measured directly. Solid lines are fits to the data using Eq. (2), with the intensity F (absorbed energy Ω) dependence of τ and K plotted in (b) and (c). Dashed lines in (b) and (c) represent the best fit to Eqs. (3). Inset to (a): Solutions of Eq. (2) for different K.

frequency phonon densities are n_0 and N_0, the subsequent time evolution of n is given by [28]

$$n(t) = \frac{\beta}{R}\left[-\frac{1}{4} - \frac{1}{2\tau} + \frac{1}{\tau}\frac{1}{1 - K\exp(-t\beta/\tau)} \right], \quad (2)$$

where K and τ are dimensionless parameters determined by the initial conditions:

$$K = \frac{\frac{\tau}{2}(\frac{4Rn_0}{\beta} + 1) - 1}{\frac{\tau}{2}(\frac{4Rn_0}{\beta} + 1) + 1}; \qquad \frac{1}{\tau} = \sqrt{\frac{1}{4} + \frac{2R}{\beta}(n_0 + 2N_0)}. \quad (3)$$

Equation (2) has three distinct regimes, depicted in the inset of Fig. 3(a). $K = 0$ corresponds to the stationary solution, when n_0 and N_0 after photoexcitation are already in quasiequilibrium (at a somewhat elevated T), i.e., $Rn_0^2 = \beta N_0$, and $n(t)$ is a step function. The regime $0 < K \leq 1$ corresponds to the situation when, following excitation, the number of QPs is higher than the quasiequilibrium value, while $-1 \leq K < 0$ represents the opposite situation when the initial T of $\omega > 2\Delta$ phonons is higher than the quasiequilibrium one. The latter situation seems to be realized for MgB_2, consistent with the analysis of the OPOP data.

At low T, when the density of thermally excited QPs and $\omega > 2\Delta$ phonons is exponentially small, the change in conductivity is proportional to the PI quasiparticle density. Therefore we can fit [35] the conductivity dynamics using Eq. (2). Best fits to the data taken at various intensities are plotted by solid lines in Fig. 3(a) showing extremely good agreement with the data. The two fitting parameters τ/β and K are plotted in Figs. 3(b) and 3(c).

Importantly, the microscopic parameters R and β can be extracted by fitting the τ/β and K versus the absorbed energy density Ω to Eqs. (3). We assume that photoexcitation with Ω creates $n_0 = p\Omega/\Delta$ QPs (with energy Δ) and $N_0 = (1 - p)\Omega/2\Delta$ high frequency 2Δ phonons, where p is the portion of Ω that initially goes to QPs. A best fit to the two data sets (dashed lines) is obtained when $p \approx 6\%$ (further supporting OPOP data analysis) giving $\beta^{-1} = 15 \pm 2$ ps, $R = 100 \pm 30$ ps^{-1} unit cell^{-1}.

In conclusion, we have presented the first femtosecond studies of photoexcited carrier dynamics in MgB_2 using OPTP and OPOP techniques. The T dependence of the SC state recovery dynamics has a similar behavior as for the cuprates [1,2,5]. The main difference is that in the cuprates τ_R is a factor of 100 shorter, which we attribute to their larger gap value, causing the dynamics (and τ_R) to be governed by the lifetime of optical phonons, instead of acoustic phonons as in MgB_2 [28]. Furthermore, we have presented the first observation of time-resolved PBD. The PBD are found to be temperature and fluence dependent, which is attributed to the initial creation of high frequency phonons, rather than QPs, and supported by detailed analysis of the PBD in terms of the Rothwarf-Taylor equations [21]. Importantly, similar physics may be responsible for the longer rise times observed in single layer cuprates ($\approx$500 fs) [4] in comparison to double layered ones ($\approx$0.1 ps) [1,2,5].

Note added in proof.—Similar results in OPOP configuration have been recently reported by Xu *et al.* [36].

This research was supported by the U.S. DOE. We wish to thank G. L. Carr, I. I. Mazin, T. Mertelj, D. Mihailovic, K. A. Müller, A. Bussmann-Holder, and J. J. Tu for valuable discussions.

[1] V.V. Kabanov *et al.*, Phys. Rev. B **59**, 1497 (1999).
[2] J. Demsar *et al.*, Phys. Rev. Lett. **82**, 4918 (1999).
[3] G. P. Segre *et al.*, Phys. Rev. Lett. **88**, 137001 (2002).
[4] M. L. Schneider *et al.*, Europhys. Lett. **60**, 460 (2002).
[5] R. D. Averitt *et al.*, Phys. Rev. B **63**, 140502(R) (2001).
[6] J. Demsar *et al.*, Phys. Rev. Lett. **83**, 800 (1999).
[7] R. D. Averitt *et al.*, Phys. Rev. Lett. **87**, 017401 (2001).
[8] J. Demsar *et al.*, Phys. Rev. Lett. **91**, 027401 (2003).
[9] J. F. Federici *et al.*, Phys. Rev. B **46**, 11 153 (1992).
[10] G. L. Carr *et al.*, Phys. Rev. Lett. **85**, 3001 (2000).
[11] J. Nagamatsu, *et al.*, Nature (London) **410**, 63 (2001).
[12] S. L. Bud'ko *et al.*, Phys. Rev. Lett. **86**, 1877 (2001).
[13] H. Kotegawa *et al.*, Phys. Rev. Lett. **87**, 127001 (2001).
[14] F. Bouquet *et al.*, Europhys. Lett. **56**, 856 (2001).
[15] F. Giubileo *et al.*, Phys. Rev. Lett. **87**, 177008 (2001).
[16] S. Souma *et al.*, Nature (London) **423**, 65 (2003).
[17] A. Y. Liu, I. I. Mazin, and J. Kortus, Phys. Rev. Lett. **87**, 087005 (2001).
[18] I. I. Mazin *et al.*, Phys. Rev. Lett. **89**, 107002 (2002).
[19] H. J. Choi *et al.*, Nature (London) **418**, 758 (2002).
[20] R. A. Kaindl *et al.*, Phys. Rev. Lett. **88**, 027003 (2001).
[21] A. Rothwarf and B. N. Taylor, Phys. Rev. Lett. **19**, 27 (1967).
[22] M. C. Nuss and J. Orenstein, in *Millimeter and Submillimeter Wave Spectroscopy of Solids*, edited by G. Grüner (Springer-Verlag, Berlin, 1998).
[23] E. Knoesel *et al.*, Phys. Rev. Lett. **86**, 340 (2001).
[24] J. T. Kindt and C. A. Schmuttenmaer, J. Chem. Phys. **110**, 8589 (1999).
[25] W. N. Kang, *et al.*, Science **292**, 1521 (2001).
[26] J. Demsar *et al.*, Int. J. Mod. Phys. **17**, 3675 (2003).
[27] The normal state dynamics are virtually T independent up to 400 K and did not change when the probe photon energy was tuned from 1.45 to 1.65 eV.
[28] A detailed analysis of OPOP data together with Rothwarf-Taylor analysis will be presented elsewhere.
[29] R. Osborn *et al.*, Phys. Rev. Lett. **87**, 017005 (2001).
[30] P. B. Allen, Phys. Rev. Lett. **59**, 1460 (1987).
[31] S. D. Brorson *et al.*, Phys. Rev. Lett. **64**, 2172 (1990).
[32] J. J. Tu *et al.*, Phys. Rev. Lett. **87**, 277001 (2001).
[33] Calculated using Eq. (10) from [30] with Eliahsberg e-ph coupling function from [34].
[34] A. A. Golubov *et al.*, J. Phys. Condens. Matter **14**, 1353 (2002).
[35] To account for the experimental resolution of $\sim$0.3 ps and the initial e-e and e-ph scattering, a convolution of Eq. (2) with 0.8 ps Gaussian was used.
[36] Y. Xu *et al.*, Phys. Rev. Lett. **91**, 197004 (2003).